Hopping Conduction in Mn Ion-Implanted GaAs Nanowires

ARTICLE *in* NANO LETTERS · AUGUST 2012

Impact Factor: 13.59 · DOI: 10.1021/nl302318f · Source: PubMed

8 AUTHORS, INCLUDING:

Waldomiro Paschoal
Lund University
5 PUBLICATIONS **44** CITATIONS
SEE PROFILE

Sandeep Kumar
Lund University
35 PUBLICATIONS **266** CITATIONS
SEE PROFILE

Christian Borschel
Jena
32 PUBLICATIONS **296** CITATIONS
SEE PROFILE

Carsten Ronning
Friedrich Schiller University Jena
275 PUBLICATIONS **4,535** CITATIONS
SEE PROFILE

NANO LETTERS

Letter

pubs.acs.org/NanoLett

Hopping Conduction in Mn Ion-Implanted GaAs Nanowires

Waldomiro Paschoal, Jr.,[†,‡,⊥] Sandeep Kumar,[†,⊥] Christian Borschel,[§] Phillip Wu,[†] Carlo M. Canali,[∥] Carsten Ronning,[§] Lars Samuelson,[†] and Håkan Pettersson*[,†,‡]

[†]Solid State Physics/The Nanometer Structure Consortium, Lund University, Box 118, SE-221 00 Lund, Sweden

[‡]Dept. of Mathematics, Physics and Electrical Engineering, Halmstad University, Box 823, SE-301 18, Halmstad, Sweden

[§]Institute for Solid State Physics, Jena University, Max-Wien-Platz 1, 07743 Jena, Germany

[∥]Division of Physics, School of Computer Science, Physics and Mathematics, Linneaus University, 39233 Kalmar, Sweden

Supporting Information

ABSTRACT: We report on temperature-dependent charge transport in heavily doped Mn^+-implanted GaAs nanowires. The results clearly demonstrate that the transport is governed by temperature-dependent hopping processes, with a crossover between nearest neighbor hopping and Mott variable range hopping at about 180 K. From detailed analysis, we have extracted characteristic hopping energies and corresponding hopping lengths. At low temperatures, a strongly nonlinear conductivity is observed which reflects a modified hopping process driven by the high electric field at large bias.

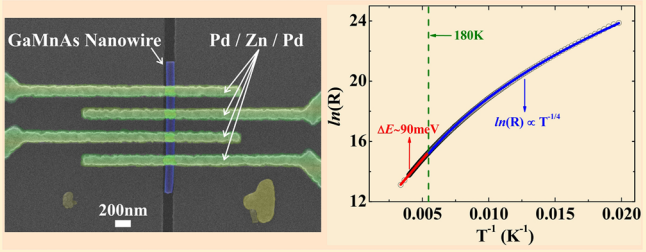

KEYWORDS: *Mott hopping, nanowires, self-assembly, ion-implantation, GaMnAs, spintronics*

A long-sought goal in electronics is the possibility to combine the two fundamental properties of spin and charge of electrons to create new devices that meet the expected requirements of computational power, data storage capacity, and communication performance in next-coming generations of electronic systems.[1] One of the most promising materials to realize such spintronic devices is $Ga_{1-x}Mn_xAs$. Mn ions incorporated into GaAs are not only responsible for magnetic moments, but they also act as acceptors providing holes that mediate ferromagnetic coupling between the Mn spins.[2−4] Most studies so far have focused on relatively high Mn concentrations to achieve a high Curie temperature, T_C. More recently, there has been an increasing interest in low-doped $Ga_{1-x}Mn_xAs$ motivated by ferromagnetic interactions in the Mott variable range hopping regime that are not well-described by any common local density carrier model.[5,6]

Semiconductor nanowires (NWs) have emerged as one of the key semiconductor technologies during recent years offering monolithic integration of III−V semiconductor nanodevices directly on a silicon chip. The flexibility in materials choice, reduced dimensions, and geometry of NWs provides unique possibilities to realize novel device families. NWs have already been considered as building blocks for nanoscale electronic and photonic devices, for example, single-electron transistors, biochemical sensors, light-emitting diodes, and solar cells.[7,8] Adding a magnetic degree of freedom to device design could potentially lead to the development of integrated 1D spintronic devices on silicon. Such a successful development requires access to high-quality single crystalline NWs with well-controlled electronic structure and magnetic properties. Up to now, it has been very difficult to realize such magnetic NWs due to segregation effects, leading to nonideal NW morphologies. Recently, we have successfully developed a new route toward heavily Mn doped single crystalline GaAs NWs via Mn^+-implantation under dynamic annealing conditions.[9] To further exploit these NWs in spintronic applications, a deeper understanding of their fundamental charge transport properties is necessary. One of the basic, yet least understood properties of $Ga_{1-x}Mn_xAs$ is the temperature dependence of the resistivity. Typical $Ga_{1-x}Mn_xAs$ samples exhibit a peak in resistivity around the Curie temperature, T_C, often with an additional weak increase in resistivity at low temperatures.[2] In less conductive samples, the aforementioned peak is less pronounced, and instead a broad resistivity shoulder is observed at T_C. While there are several reports on transport properties of bulk and thin film $Ga_{1-x}Mn_xAs$,[1,5,6,10] there is hardly any report on temperature-dependent transport measurements on $Ga_{1-x}Mn_xAs$ NWs. Previously reported quantum transport studies of ZnO[11] and InN[12] NWs showed that the conduction at low temperatures is dominated by a hopping mechanism. The absence of corresponding reports on $Ga_{1-x}Mn_xAs$ NWs most likely reflects the previously mentioned difficulties to grow single crystalline NWs with conventional techniques. In reduced-dimensional systems, it is expected that new features different from the bulk counterpart will arise. The Mn doped GaAs NWs are nearly ideal systems to investigate 1D transport mechanisms and localization related effects.

Received: June 21, 2012
Revised: August 3, 2012

   dx.doi.org/10.1021/nl302318f | *Nano Lett.* XXXX, XXX, XXX−XXX

In this Letter, we present significant insight into the hole transport properties of heavily doped Mn^+-implanted $Ga_{1-x}Mn_xAs$ NWs. From meticulous measurements of the temperature-dependent resistance, in combination with detailed analysis, it is shown that the transport is governed by different hopping mechanisms within an impurity band of localized Mn states. With decreasing temperature, there is a clear transition from nearest neighbor hopping (NNH) to Mott variable range hopping (VRH) conduction. It is also shown that electric field driven VRH dominates at low temperatures and high electric field strengths.

Single crystalline GaAs NWs of diameter 80 nm were grown by MOVPE using monodisperse Au particles as a catalyst.[13] To optimize the implantation angle, the NWs were grown on GaAs (001) substrates leading to an inclined growth direction of 35° toward the substrate. The as-grown NWs were subsequently implanted with 100 keV Mn^+ using a general purpose implanter (High Voltage Engineering Europa). The selected implantation dose of 1.8×10^{16} ions/cm^2 resulted in a Mn concentration of 2.5% (corresponding to a stoichiometry of $Ga_{1-x}Mn_xAs$ with $x = 0.05$) as determined by transmission electron microscopy (TEM)/energy-dispersive spectrometry (EDS). Results from computer simulations of the implanted ion profile, using our own developed *iradina* code,[14] show that this implantation energy leads to a fairly homogeneous concentration of Mn in the GaAs NWs. We have previously reported that the imposed dynamic annealing conditions during implantation lead to high crystalline quality and ideal NW morphology after implantation.[9] For transport measurements, NWs were mechanically transferred onto a silicon substrate covered by a 210 nm thick silicon dioxide layer on which reference markers and macroscopic metal pads were predefined. Electron beam lithography (EBL) was used to define contacts connecting individual NWs to the macroscopic contact pads. The NWs were etched in HCl/H_2O solution for 20 s, followed by a 2 min surface passivation in a heated (40 °C) NH_4S_x/H_2O solution. The Ohmic contacts to the NWs were made by evaporating Pd (2 nm)/Zn (20 nm)/Pd (83 nm) after etching and passivation. The sample processing was finalized by a lift-off process. To investigate the possible influence of contact resistance, 2-probe and 4-probe measurements were compared. From these measurements we conclude that the contact resistance is negligible compared to the NW resistance at all temperatures (Figure S1 of the Supporting Information). The transport measurements were performed in a Janis VariTemp superconducting cryomagnet system (model 8T-SVM).

Figure 1 shows current voltage (I–V) characteristics of a single $Ga_{0.95}Mn_{0.05}As$ NW. At room temperature, the slightly nonlinear and antisymmetric I–V curve suggests that the transport could be governed by incoherent hole hopping between spatially adjacent energy states in the impurity band formed by the Mn^+ implantation.[15] The expected current versus bias relation for such a hopping process is given by

$$I \sim \sinh\left(\frac{AV}{k_B T}\right) \quad (1)$$

where A is a constant which depends on the hopping distance and the distance between the contacts on the NW. For $T > 50$ K, all I–V curves could be perfectly fitted by eq 1 above. At lower temperatures, the I–V curves become increasingly nonlinear, however with maintained antisymmetry with respect to the bias (Figure 1, lower inset). To further unravel the

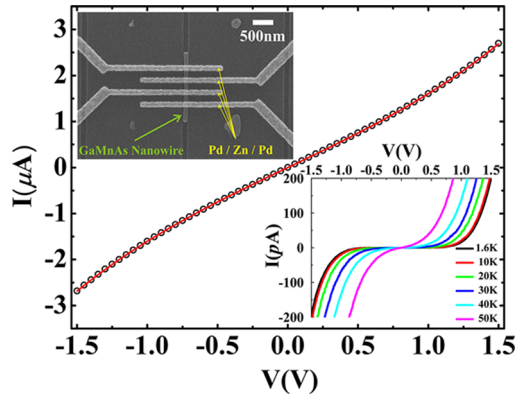

Figure 1. Current–voltage (I–V) characteristics of a single $Ga_{1-x}Mn_xAs$ NW ($x = 0.05$) at room temperature. Circles are the experimental data, while the red solid curve is a fitting to eq 1. The lower inset shows the strongly nonlinear I–V characteristics at lower temperatures. The upper inset shows an SEM micrograph of a NW with contacts for 4-point resistance measurements.

electronic transport mechanism of the NWs, we study the temperature dependence of the resistance of our devices from 1.6 to 300 K. Figure 2 shows the resistance (R) versus

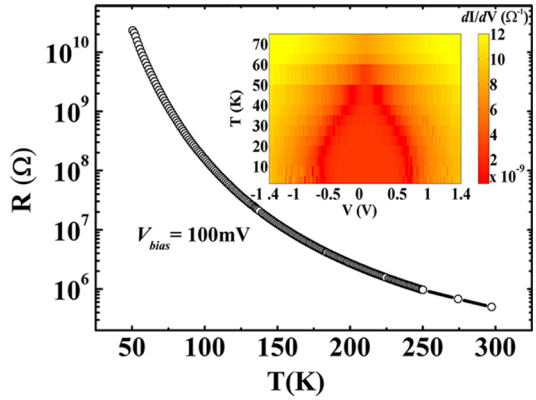

Figure 2. Resistance dependence on the temperature at a bias of 0.1 V. The inset shows the differential conductance (dI/dV) as a function of bias and temperature.

temperature (T) plot in the temperature range 50–300 K for a single $Ga_{0.95}Mn_{0.05}As$ NW at a constant bias $V = 0.1$ V within the linear region of the I–V curve. The NWs exhibit a high resistance of about 0.5 MΩ at 300 K, which increases by 4 orders of magnitude as the temperature is decreased to 50 K. In a constant mobility drift model, the room temperature resistance of 0.5 MΩ corresponds to a hole concentration of 2.0×10^{17} cm^{-3}, assuming a reduced hole mobility of 30 cm^2·V^{-1}·s^{-1} [16] and a 80 nm NW diameter. This value of the hole mobility is taken from studies of p-doped GaAs NWs[14] with slightly larger NW diameters. We do not exclude the possibility that the effective hole mobility in our samples could be smaller, yielding a larger hole concentration than what stated above. Note however that the value reported here is consistent with the hole concentration extracted with a different method in $Ga_{1-x}Mn_xAs$ NWs similar to the ones studied in this work.[17] In our estimate, we have neglected any influence of, for example, Fermi level pinning at the surface of the NW. The hole density is much lower than expected considering the 2.5% Mn detected with EDS. Possible reasons for the low carrier

dx.doi.org/10.1021/nl302318f | *Nano Lett.* XXXX, XXX, XXX–XXX

concentration include, for example, compensation due to interstitial Mn impurities and As antisites created by the ion implantation.

To investigate the bias dependence of the conductance more in detail, we plot the differential conductance dI/dV as a function of both T and applied bias V in Figure 2 (inset). The conductance due to thermally activated hopping falls below the detection limit at 0.1 V bias below 50 K. It is noted that no features revealing the metal-to-insulator transition, generally observed near T_C in weakly metallic $Ga_{1-x}Mn_xAs$, are observed in Figure 2. At all measured temperatures and applied biases, an insulating behavior ($dR/dT < 0$) is indeed observed. Different transport mechanisms have been proposed in the literature for doped semiconductors.[15] For a p-type semiconductor at low temperatures, most of the free holes are recaptured by the acceptors. As a result, hole conduction in the valence band becomes less important, and hole hopping directly between acceptors in the impurity band provides the main contribution to the conductivity. The hopping conduction is associated with hole jumping from occupied acceptors to empty ones. Hopping conductivity is governed by the hopping probability between impurity sites. A hopping hole will always try to find the lowest activation energy ΔE, given by the energy separation between adjacent Mn-related states, and the corresponding shortest hopping distance. There is an optimum hopping distance r, which maximizes the hopping probability. At thermal equilibrium (zero bias), the hopping probability is given by

$$P \sim \exp(-2r/a - \Delta E/k_B T) \tag{2}$$

where k_B is the Boltzmann constant and a is the localization length of the hole wave function in the impurity band. The hopping distance r, which can be much longer than the localization length at low temperatures,[18] depends on the temperature according to

$$r = [9a/(8\pi N(E_F)k_B T)]^{1/4} \tag{3}$$

for a 3D system. Here $N(E_F)$ is the density of states near the Fermi level. The corresponding activation energy is given by

$$\Delta E = 3/[4\pi r^3 N(E_F)] \tag{4}$$

At elevated temperatures, r eventually becomes equal to the nearest neighbor distance d. The hopping probability then becomes

$$P \sim \exp(-\Delta E_A/k_B T) \tag{5}$$

which resembles an Arrhenius relation describing a nearest-neighbor hopping mechanism with an activation energy ΔE_A. According to the theory of VRH proposed by Mott,[19,20] if the effect of electron−electron interactions is negligible, and a constant $N(E_F)$ is assumed, the temperature dependence of the resistance in the linear (Ohmic) region can be expressed as

$$R = R_0 \exp\left[\frac{T_0}{T}\right]^p \tag{6}$$

where $p = 1/4$, $1/3$, or $1/2$ for 3D, 2D, and 1D systems, respectively. Here R_0 and T_0 denote materials parameters. The exponent p in eq 6 is precisely determined by the slope of the double logarithmic plot of $W = d(\log(G))/d(\log(T))$ versus T, where $G = 1/R$ is the conductance of the NW.[21] As shown in the lower inset of Figure 3, a change of slope of $\log(d(\log(G))/d(\log(T)))$ versus $\log(T)$ is observed around 180 K. The value of p amounts to about 0.25 in the temperature region 50 K < T < 180 K and 0.9 above 180 K, respectively. A value $p = 0.25$ corresponds to 3D Mott VRH, whereas $p = 0.9$ is consistent with a NNH mechanism.

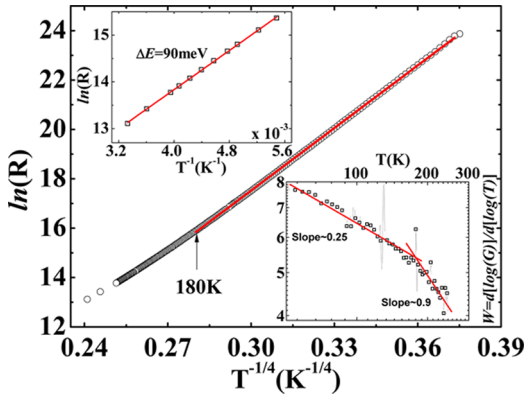

Figure 3. Resistance fitted (red solid line) to the Mott VRH model with $p = 1/4$ (eq 6) in the temperature range 50 K < T < 180 K. Upper inset: Arrhenius plot of the resistance data in the temperature interval 180 K < T < 300 K. Lower inset: Plot of d log(G)/d log(T) versus T, where the red solid fitting lines were used to extract the p-factors.

From the R versus T behavior, several characteristic parameters describing the charge transport in NWs can be extracted. The $\ln(R)$ versus $T^{-1/4}$ plot for $Ga_{0.95}Mn_{0.05}As$ NWs is shown in Figure 3. From the slope of the curve between 50 and 180 K, the fitting parameter T_0 can be estimated. T_0 is related to the hole localization length a and density of states near the Fermi level $N(E_F)$ according to

$$T_0 = 18/k_B a^3 N(E_F) \tag{7}$$

From the slope of the linear fit to $\ln(R)$ versus $T^{-1/4}$ curve in Figure 3, we deduce a value of $T_0 = 5.2 \times 10^7$ K, which corresponds to a $N(E_F) = 4.0 \times 10^{18}$ (eV·cm^3)$^{-1}$. The value of a is assumed to be of the same order as the acceptor Bohr radius for Mn in GaAs (~1 nm). From eqs 3 and 4 we deduce an average hopping energy ΔE of 34 meV and a hopping length of $r = 12.0$ nm at 50 K. At 180 K, ΔE increases to 90 meV while the hopping length decreases to 8.7 nm. The finding of such large hopping lengths, particularly at relatively high temperatures, is puzzling. Within a single-particle hopping scenario the hopping length r should eventually become of the order of the average impurity distance. At the moment we have no satisfactory explanation of this result. As already mentioned, the low carrier concentration, which at first hand indeed would imply a large distance between the hopping sites, most likely reflects efficient compensation due to interstitial Mn impurities and As antisites created by the ion implantation. More detailed investigations are needed to unravel the hopping processes through an impurity band influenced by these impurity states. Moreover, recent studies investigating the prototype ferromagnetic semiconductor $Ga_{1-x}Mn_xAs$ shows that our understanding of the electronic structure in samples in relatively high doping regimes is still far from complete.[22] In particular, some of these measurements seem to suggest that all of the acceptor holes might reside in states generated by the Mn impurities.[23] Hopping processes in the presence of many localized nearby holes might differ substantially from the usual single-particle hopping scenario, and correlation effects might not be excluded. Our consistent finding of larger than expected hopping distances might signal a problematic attempt of

dx.doi.org/10.1021/nl302318f | Nano Lett. XXXX, XXX, XXX−XXX

analyzing a correlated system with a single-particle scheme. Similar indications occur also when studying thermoelectric effects in similar samples.[17] Above 180 K, the NNH mechanism dominates with activation energy of 90 meV. The Arrhenius plot is shown in Figure 3 (upper inset). The extracted p-factor of 0.9 for $T > 180$ K is close to 1 also valid for valence band conduction. We thus cannot exclude a contribution to the conductivity from holes excited to the valence band. The NWs used here have a diameter of ∼80 nm, which is much larger than the hopping length, so the hole transport reveals mainly three-dimensional character. At low temperatures (< 50 K) the conduction mechanism of VRH is modified at large biases. Under high electric field conditions, a hole can jump from a filled state to an empty state along the field direction with an activation energy reduced by an amount eEr.[24,25] When the electric field reaches a critical value E_C, such that the energy eE_Cr gained during a hop becomes comparable to the activation energy for hopping, holes can move along the field. The resistance which becomes temperature independent can then be expressed in the form

$$R = R_{0E} \exp\left[\frac{E_0}{E}\right]^p \quad (8)$$

where R_{0E} and E_0 are materials constants. E_0 is proportional to T_0 as

$$E_0 = (k_B T_0/2ea) \quad (9)$$

where a is the localization length as stated before.

In Figure 4, we have plotted ln R versus $E^{-1/4}$. It is readily observed that the curves at different temperatures merge on a single line at a temperature-dependent E_C. From the slope of this line, we deduce $E_0 = 2.0 \times 10^{12}$ V·m^{-1}. Inserting the values of E_0 and T_0 into eq 9 gives the localization length $a = 1.1$ nm, which is in very good agreement with the expected Mn acceptor Bohr radius.

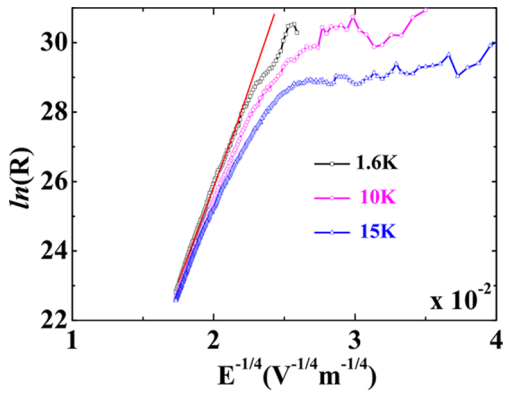

Figure 4. Resistance as a function of electric field and temperature. The red solid line is a least-squares fit to the high-field data.

In conclusion, we have reported on detailed temperature-dependent resistance measurements and $I-V$ characteristics of heavily Mn^+-implanted single crystalline $Ga_{0.95}Mn_{0.05}As$ NWs. Whereas TEM confirms that the NWs are single crystalline, the electrical data exhibit clear evidence of disorder. The transport is governed by variable range hopping at lower temperatures (50 K < T < 180 K) with a crossover to nearest neighbor hopping at about $T > 180$ K. The extracted values of optimal hopping distance are considerably larger than the average impurity separation, even at high temperatures ($T \sim 180$ K), suggesting that correlation effects beyond a single-particle picture might be at play. At low temperatures and high electric field strengths, signs of field-induced variable range hopping are revealed. These fundamental studies provide critical insight into the transport mechanisms likely to be found in next-generations of integrated nanoscale electronic devices compatible with main-stream silicon technology.

■ ASSOCIATED CONTENT

Supporting Information

Current−voltage characteristics measured with 2-probe and 4-probe geometry. This material is available free of charge via the Internet at http://pubs.acs.org.

■ AUTHOR INFORMATION

Corresponding Author

*E-mail: hakan.pettersson@hh.se.

Author Contributions

⊥These authors contributed equally to this work and are cofirst authors.

Notes

The authors declare no competing financial interest.

■ ACKNOWLEDGMENTS

The authors acknowledge financial support from the Swedish Research Council, the Knut and Alice Wallenberg Foundation, the Swedish National Board for Industrial, Technological Development, the Swedish Foundation for Strategic Research and the Nordforsk research network “Nanospintronics; theory and simulations”. One of the authors, W.P., Jr., gratefully acknowledges financial support from the Pará Education Secretary (SEDUC) and the Pará Government School (EGPA).

■ REFERENCES

(1) Ohno, H. *Science* **1998**, *281*, 951.
(2) Dietl, T. *Semicond. Sci. Technol.* **2002**, *17*, 377.
(3) MacDonald, A. H.; Schiffer, P.; Samarth, N. *Nat. Mater.* **2005**, *4*, 195.
(4) Ohno, H.; Chiba, D.; Matsukura, F.; Omiya, T.; Abe, E.; Dietl, T.; Ohno, Y.; Ohtani, K. *Nature* **2000**, *408*, 944.
(5) Dobrowolska, M.; Tivakornsasithorn, K.; Liu, X.; Furdyna, J. K.; Berciu, M.; Yu, K. M.; Walukiewicz, W. *Nat. Mater.* **2012**, *11*, 444.
(6) Sheu, B. L.; Myers, R. C.; Tang, J.-M.; Samarth, N.; Awschalom, D. D.; Schiffer, P.; Flatté, M. E. *Phys. Rev. Lett.* **2007**, *99*, 227205.
(7) Cui, Y.; Wei, Q.; Park, H.; Lieber, C. M. *Science* **2001**, *293*, 1289.
(8) Thelander, C.; Mårtensson, T.; Björk, M. T.; Ohlsson, B. J.; Larsson, M. W.; Wallenberg, L. R.; Samuelson, L. *Appl. Phys. Lett.* **2003**, *83*, 2052.
(9) Borschel, C.; Messing, M. E.; Borgström, M. T., Jr.; W., P.; Wallentin, J.; Kumar, S.; Mergenthaler, K.; Deppert, K.; Canali, C. M.; Pettersson, H.; Samuelson, L.; Ronning, C. *Nano Lett.* **2011**, *11*, 3935.
(10) Kyrychenko, F. V.; Ullrich, C. A. *Phys. Rev. B* **2009**, *80*, 205202.
(11) Ma, Y. J; Zhang, Z.; Zhou, F.; Lu, L.; Jin, A.; Gu, C. *Nanotechnology* **2005**, *16*, 746.
(12) Huang, L.; Li, D.; Chang, P.; Chu, S.; Bozler, H.; Beloborodov, I. S.; Lu, J. G. *Phys. Rev. B* **2011**, *83*, 245310.
(13) Mikkelsen, A.; Sköld, N.; Ouattara, L.; Borgström, M. T.; Andersen, J. N.; Samuelson, L.; Seifert, W.; Lundgren, E. *Nat. Mater.* **2004**, *3*, 519.
(14) Borschel, C.; Ronning, C. *Nucl. Instrum. Methods Phys. Res., Sect. B* **2011**, *269*, 2133.
(15) Singh, J. *Physics of semiconductors and their heterostructures*; McGraw-Hill, Inc.: New York, 1993.
(16) Ketterer, B.; Uccelli, E.; Morral, A. F. *Nanoscale* **2012**, *4*, 1789.

(17) Wu, P.; Paschoal, W., Jr.; Kumar, S.; Borschel, C.; Ronning, C.; Canali, C. M.; Samuelson, L.; Pettersson, H.; Linke, H. *J. Nanotechnol.*, submitted.
(18) Shklovskii, B. I.; Efros, A. L. *Electronic properties of doped semiconductors*, Springer-Verlag, Inc.: New York, 1984.
(19) Mott., N. F. *Philos. Mag.* **1969**, *19*, 835.
(20) Lee, P. A. *Rev. Mod. Phys.* **1985**, *57*, 287.
(21) Zabrodskii, A. G. *Philos. Mag.* **2001**, *81*, 1131.
(22) Ohya, S.; Takata, K.; Tanaka, M. *Nat. Phys.* **2011**, *7*, 342.
(23) Flatté, M. E. *Nat. Phys.* **2011**, *7*, 285.
(24) Shahar, D.; Ovadyahu, Z. *Phys. Rev. Lett.* **1990**, *64*, 2293.
(25) Yu, D.; Wang, C.; Wehrenberg, B. L.; Guyot-Sionnest, P. *Phys. Rev. Lett.* **2004**, *92*, 216802.

dx.doi.org/10.1021/nl302318f | *Nano Lett.* XXXX, XXX, XXX−XXX